LETTER

Unusual upper critical fields of the topological nodal-line semimetal candidate $Sn_xNbSe_{2-\delta}$

IOP ebooks™

Bringing together innovative digital publishing with leading authors from the global scientific community.

Start exploring the collection−download the first chapter of every title for free.

Letter

Unusual upper critical fields of the topological nodal-line semimetal candidate $Sn_xNbSe_{2−\delta}$

Riffat Munir[1], K A M Hasan Siddiquee[1], Charuni Dissanayake[1], Xinzhe Hu[2], Yasumasa Takano[2], Eun Sang Choi[3] and Yasuyuki Nakajima[1,*]

[1] Department of Physics, University of Central Florida, Orlando, Florida 32816, United States of America
[2] Department of Physics, University of Florida, Gainesville, Florida 32611, United States of America
[3] National High Magnetic Field Laboratory, Florida State University, Tallahassee, Florida 32310, United States of America

E-mail: yasuyuki.nakajima@ucf.edu

CrossMark

Abstract

We report superconductivity in $Sn_xNbSe_{2−\delta}$, a topological nodal-line semimetal candidate with a noncentrosymmetric crystal structure. The superconducting transition temperature T_c of this compound is extremely sensitive to Sn concentration x and Se deficiency δ, 5.0 K for $Sn_{0.13}NbSe_{1.70}$ and 8.6 K for $Sn_{0.14}NbSe_{1.71}$ and $Sn_{0.15}NbSe_{1.69}$. In all samples, the temperature dependence of the upper critical field $H_{c2}(T)$ differs from the prediction of the Werthamer–Helfand–Hohenberg theory. While the zero-temperature value of the in-plane upper critical field of $Sn_xNbSe_{2−\delta}$ with the higher T_c is lower than the BCS Pauli paramagnetic limit H_P, that of the lower T_c sample exceeds H_P by a factor of $\sim$2. Our observations suggest that a possible odd-parity contribution dominates the superconducting gap function of $Sn_xNbSe_{2−\delta}$, and it can be fine-tuned by the Sn concentration and Se deficiency.

S Supplementary material for this article is available online

(Some figures may appear in colour only in the online journal)

Topological superconductors, characterized by a topologically nontrivial gapped state in the bulk with gapless surface states [1], have attracted great interest because of potential applications to topologically protected quantum computing [2, 3]. Such nontrivial gapped states can be stabilized by odd-parity Cooper pairing, occasionally realized in noncentrosymmetric superconductors with strong spin-orbit coupling. The lack of inversion symmetry in the crystal structures allows superposition of spin singlet (even parity) and spin triplet (odd parity) in superconducting gap functions. This mixing of parity can be fine-tuned by the spin-orbit coupling strength, as observed in the crossover from even to odd-parity pairing states in $Li_2(Pd,Pt)_3Bi$ as the Pt concentration is varied [4]. Hence, the search for noncentrosymmetric superconductors with strong spin-orbit coupling serves as one of the routes toward the realization of topological superconductivity. The

* Author to whom any correspondence should be addressed.

noncentrosymmetric $AB\mathrm{Se}_2$ (A = Sn or Pb and B = Nb or Ta) family is a promising candidate for a topological superconductor. Recent experimental studies have revealed superconductivity in PbTaSe_2 at T_c = 3.8 K [5, 6], with a fully opened superconducting gap probed by various measurements, including specific heat [7], thermal conductivity [8], and penetration depth measurements [9]. Moreover, angle-resolved photoemission spectroscopy has identified this materials as a topological nodal-line semimetal with drumhead surface states [10, 11]. Although the parity of the superconducting pairing state is yet to be determined, the lack of inversion symmetry along with the nontrivial topological band structure can induce topological superconductivity in this system in PbTaSe_2.

In addition to this compound, PbNbSe_2, SnNbSe_2, and SnTaSe_2 are predicted by *ab-initio* calculations to be superconductors with nontrivial topological nodal lines in the band structure [12]. According to the calculations, the superconducting transition temperatures, T_c, of these materials are expected to be higher than that of PbTaSe_2, and notably, the predicted T_c of SnNbSe_2 is 7 K, suggestive of a possible realization of topological superconductivity in this material with a relatively high T_c, compared with known bulk topological superconductor candidates, such as half Heusler compounds YPtBi (T_c = 0.6 K) [13] and YPdBi (T_c = 1.6 K) [14], In-doped SnTe (T_c = 1.2 K) [15], metal-intercalated $\mathrm{Bi}_2\mathrm{Se}_3$ (T_c = 3.2 K) [16–18], and β-$\mathrm{Bi}_2\mathrm{Pd}$ (T_c = 5.4 K) [19, 20]. The higher T_c can be advantageous to detect Majorana bound sates with the energy spacing Δ^2/E_F, where Δ and E_F are the superconducting gap and Fermi energy, respectively, and can eliminate one bottleneck in the exploration for topological superconductivity [21].

We here report unusual superconductivity in $\mathrm{Sn}_x\mathrm{NbSe}_{2-\delta}$, which retains the noncentrosymmetric crystal structure of stoichiometric $AB\mathrm{Se}_2$. Although theoretical predictions specific to this compound are presently lacking, we propose by analogy to stoichiometric $AB\mathrm{Se}_2$ that $\mathrm{Sn}_x\mathrm{NbSe}_{2-\delta}$ can be a promising candidate for a topological nodal-line semimetal. The superconducting transition temperature of $\mathrm{Sn}_x\mathrm{NbSe}_{2-\delta}$ varies with Sn concentration and Se deficiency—up to 8.6 K, a relatively high T_c among bulk topological superconductor candidates known to date. The measured upper critical fields of $\mathrm{Sn}_x\mathrm{NbSe}_{2-\delta}$ cannot be described by the Werthamer–Helfand–Hohenberg (WHH) theory for conventional type-II superconductors [22], and the zero-temperature value of the upper critical field for $\mathrm{Sn}_{0.13}\mathrm{NbSe}_{1.70}$ exceeds the BCS Pauli paramagnetic limit by a factor of $\sim$2. The unusual temperature dependence of the upper critical fields and the enhancement beyond the Pauli paramagnetic limit suggest that a possible odd-parity component dominates the superconducting gap function of $\mathrm{Sn}_x\mathrm{NbSe}_{2-\delta}$, indicating that this compound is a promising candidate for realizing topological superconductivity.

Single crystals of $\mathrm{Sn}_x\mathrm{NbSe}_{2-\delta}$ were grown by using a self-flux method. A mixture of NbSe_2 and Sn in the ratio of NbSe_2:Sn = 1:2—6 was sealed in a quartz tube, heated up to 900°C, kept for 2–3 days, and slowly cooled down to 600°C. The excess of molten Sn flux was removed by centrifuging.
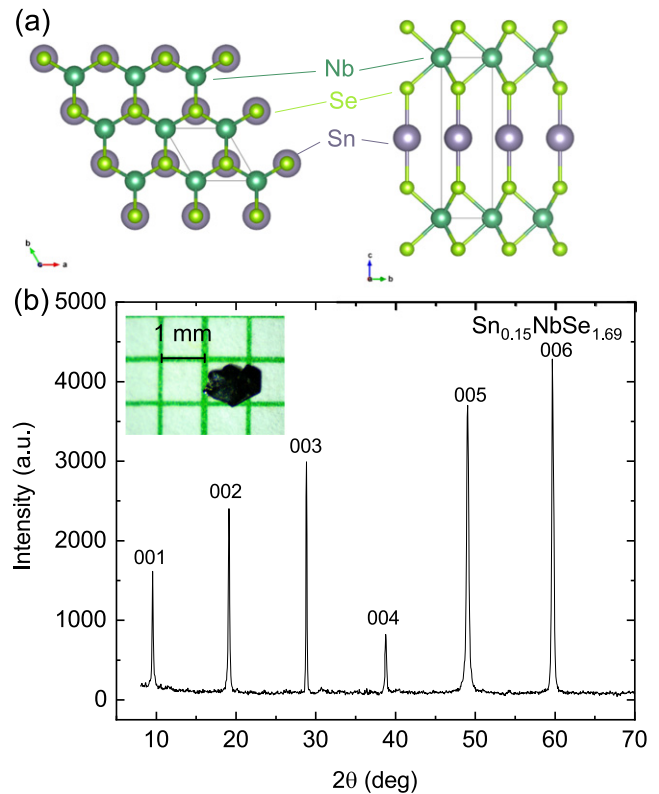

Figure 1. Crystal structure and x-ray diffraction pattern of $\mathrm{Sn}_x\mathrm{NbSe}_{2-\delta}$. (a) Top view (left panel) and side view (right panel) of the crystal structure of SnNbSe_2 with the space group $P\bar{6}m2$ [23]. (b) X-ray diffraction pattern for single crystal $\mathrm{Sn}_{0.15}\mathrm{NbSe}_{1.69}$ measured with Cu K_α radiation. We only observe (00ℓ) Bragg peaks from the ab plane. The obtained lattice constant c is 9.2976(12) Å. Inset: optical image of a $\mathrm{Sn}_x\mathrm{NbSe}_{2-\delta}$ single crystal. The typical crystal size is $\sim$ 1 × 1 × 0.3 mm^3.

The typical size of obtained flake-like crystals is about $1 \times 1 \times 0.3$ mm^3.

Our measured single-crystal x-ray diffraction pattern is consistent with the noncentrosymmetric crystal structure of SnNbSe_2 with the space group $P\bar{6}m2$. As shown in figure 1(b), we observed only (00ℓ) reflections, which yielded the lattice constant c = 9.2976(12) Å close to the reported value of 9.30 Å for polycrystalline SnNbSe_2 [24]. The atomic ratio of the crystals was found to be Sn:Nb:Se = 0.11–0.15:1:1.60–1.74 with x-ray fluorescence spectroscopy, suggestive of slightly intercalated Sn and deficiency of Se. Although the Sn concentrations in our samples are only 11%–15% of the stoichiometric value, the identified crystal structure is the same as that of $AB\mathrm{Se}_2$ and different from the 2H–NbSe_2-type structure of Sn-intercalated NbSe_2 with x up to 0.04 [25].

We reveal superconductivity in $\mathrm{Sn}_x\mathrm{NbSe}_{2-\delta}$ with resistivity measurements from 300 K down to 2 K. Figure 2(a) shows a typical temperature dependence of the resistivity of $\mathrm{Sn}_x\mathrm{NbSe}_{2-\delta}$. The resistivity at T = 300 K is about 700 $\mu\Omega$ cm. Upon cooling, the resistivity shows metallic behavior, followed by a superconducting transition at low temperatures (figure 2(a)). The superconducting transition temperatures T_c, determined by the midpoint of resistive transitions, are 5.0 K for $\mathrm{Sn}_{0.13}\mathrm{NbSe}_{1.70}$ and 8.6 K for
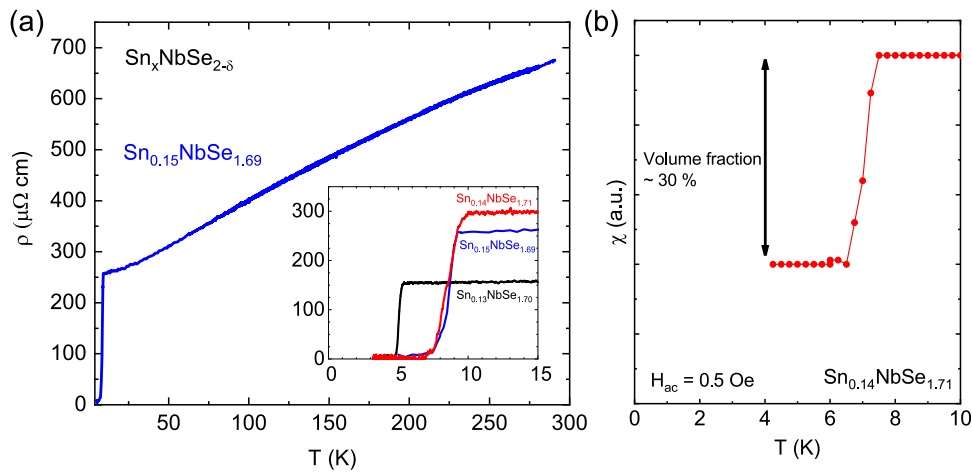
Figure 2. Temperature dependence of the resistivities and ac susceptivity of $Sn_xNbSe_{2-\delta}$. (a) Overall temperature dependence of the resistivity of $Sn_{0.15}NbSe_{1.69}$. Preceded by metallic behavior, $Sn_xNbSe_{2-\delta}$ undergoes a superconducting transition at low temperatures. The residual resistivity ratio $RRR = \rho(300\,K)/\rho(T_c)$ is 2.3–3.0, suggestive of abundant disorder. Inset: low temperature resistivities of $Sn_xNbSe_{2-\delta}$, indicating superconducting transitions at 5.0 K for $Sn_{0.13}NbSe_{1.70}$ and 8.6 K for $Sn_{0.14}NbSe_{1.71}$ and $Sn_{0.15}NbSe_{1.69}$. (b) Temperature dependence of ac susceptibility. The superconducting volume fraction determined by the calibration using tin is about 30%.

$Sn_{0.14}NbSe_{1.71}$ and $Sn_{0.15}NbSe_{1.69}$ (figure 2(a) inset). In contrast, no superconductivity has been observed down to 1.5 K in polycrystalline $Sn_{2/3}NbSe_2$ [26]. We observe Meisner screening at low temperatures starting at $T \sim 7$ K, where the resistivity becomes zero in $Sn_{0.14}NbSe_{1.71}$ (figure 2(b)). The superconducting volume fraction determined by a calibration using tin is ∼30%, comparable to typical volume fractions achieved by early works on $Cu_xBi_2Se_3$ [16, 17]. It has been pointed out that sample qualities of $ABSe_2$ can be correlated with the presence of stacking faults [7], which is in fact supported by our powder x-ray diffraction result (see supplementary material (https://stacks.iop.org/JPCM/33/23LT01/mmedia)). The imperfect volume fraction found in our sample suggests that stacking faults may, by affecting local stoichiometry, be causing some regions to remain nonsuperconducting.

The normal-state resistivity of $Sn_xNbSe_{2-\delta}$ right above T_c is much higher than that of $PbTaSe_2$. Because of this high residual resistivity, the values of the residual resistivity ratio RRR = $\rho(300\,K)/\rho(T_c)$ are 2.3 for $Sn_{0.13}NbSe_{1.70}$, 2.7 for $Sn_{0.14}NbSe_{1.71}$, and 3.0 for $Sn_{0.15}NbSe_{1.69}$, 30–50 times as small as that of single-crystal $PbTaSe_2$ [6, 7, 27]. Interestingly, despite the high residual resistivity, or the low RRR, the T_c of 8.6 K not only surpasses the theoretical prediction of 7 K [12] but also those of most known topological superconductor candidates.

To determine the upper critical fields of $Sn_xNbSe_{2-\delta}$, we measured the resistivity in a 35 T resistive magnet equipped with a ^{3}He cryostat at the National High Magnetic Field Laboratory in Tallahassee, Florida. We show magnetoresistance of $Sn_xNbSe_{2-\delta}$ in two different magnetic field configurations: $H \parallel I \parallel ab$ (in-plane configuration) and $H \perp ab, I \parallel ab$ (out-of-plane configuration). For both field configurations and in both $Sn_{0.13}NbSe_{1.70}$ and $Sn_{0.14}NbSe_{1.71}$, the magnetoresistance is indiscernible even at an applied magnetic field of 35 T

(figure 3), indicative of short mean free paths of charge carriers due to disorder caused most likely by slightly intercalated Sn and deficiency of Se. On the other hand, we find a notable difference in the anisotropy of upper critical fields, $\Gamma = H_{c2}^{ab}/H_{c2}^c$, between these two samples. In the out-of-plane configuration for $Sn_{0.13}NbSe_{1.70}$ (figure 3(b)), the upper critical field parallel to the c axis, H_{c2}^c, defined by the midpoints of sharp resistive transitions, is 5 T at 0.3 K. In the in-plane configuration for $Sn_{0.13}NbSe_{1.70}$ (figure 3(a)), the transition widths are broad, and the upper critical field parallel to the ab plane, H_{c2}^{ab}, is extremely high, extracted to be 15 T at 0.3 K. These values of H_{c2} yield a large anisotropy of the upper critical field, $\Gamma = 3$, for $Sn_{0.13}NbSe_{1.70}$. In contrast, we observe similar transition widths with very similar H_{c2} in both field configurations for $Sn_{0.14}NbSe_{1.71}$, suggestive of a nearly isotropic upper critical field with $\Gamma = 1.1$ (figures 3(d) and (e)). In the isostructural compound $PbTaSe_2$, the anisotropy of H_{c2} is measured to be 11.6 [6], much larger than the observed anisotropy in $Sn_xNbSe_{2-\delta}$, although the two compounds share similar electronic band structures [12]. The striking difference in the upper critical fields and the transition temperatures between $Sn_{0.13}NbSe_{1.70}$ and $Sn_{0.14}NbSe_{1.71}$ may be correlated with carrier densities determined by the Sn concentration and Se deficiency. A slight change in the carrier densities can cause a drastic change in superconducting properties and may even induce a superconducting pairing symmetry transition.

We also measured in-plane anisotropy of the upper critical field in $Sn_{0.13}NbSe_{1.70}$. As shown in figure 3(c), magnetoresistance at fields parallel to the ab-plane but perpendicular to the applied current shows broad transitions accompanied by kinks indicated by black arrows. The upper critical fields in this configuration, determined by 50% of resistive transitions, are slightly lower than those in the configuration for $H \parallel I \parallel ab$, as can be seen in figure 3(a), suggesting a discernible in-plane anisotropy.

Figure 3(f) shows the Hall resistivity ρ_{yx} of $Sn_{0.11}NbSe_{1.60}$ in the normal state. The Hall resistivity is positive and perfectly

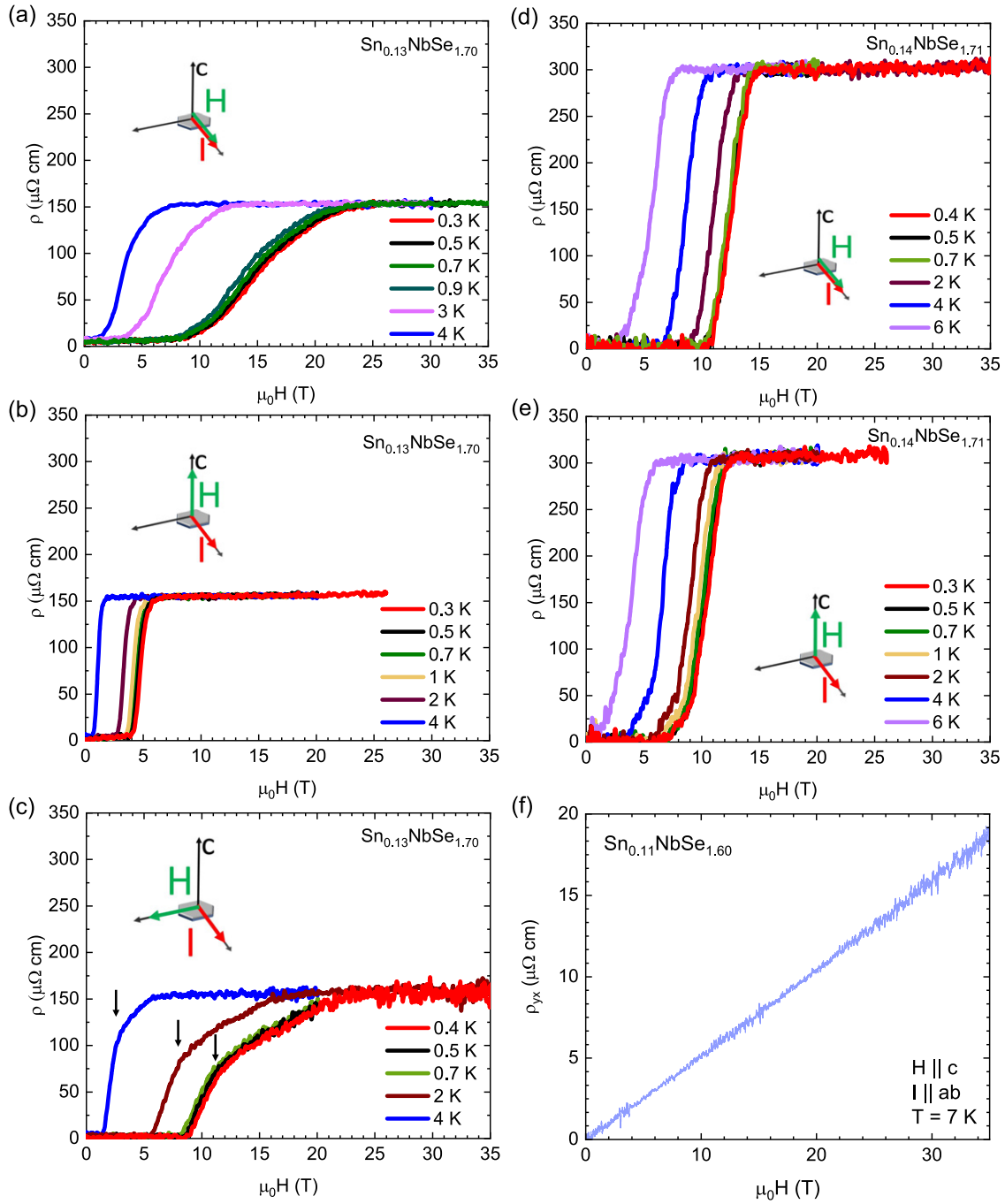**Figure 3.** Magnetotransport in $Sn_xNbSe_{2-\delta}$. Resistivity of $Sn_{0.13}NbSe_{1.70}$ as a function of magnetic fields parallel to (a) the *ab* plane and (b) the *c* axis at several temperatures. Electrical current is applied in the *ab* plane. While the resistive transitions for $H \parallel c$ are sharp, the transitions for $H \parallel ab$ are broad. The upper critical fields obtained by the midpoints of the resistive transitions show high anisotropy $\Gamma = H_{c2}^{ab}/H_{c2}^{c} = 3$ in $Sn_{0.13}NbSe_{1.70}$. (c) Transverse magnetoresistance of $Sn_{0.13}NbSe_{1.70}$ in magnetic fields parallel to the *ab* plane. The resistive transitions are broad, and show kinks indicated by arrows, associated with vortex motion due to the Lorentz force. The extracted H_{c2}^{ab} for $H \perp I$ is slightly lower than H_{c2}^{ab} for $H \parallel I$, obtained from the curves shown in panel (a). Resistivity of $Sn_{0.14}NbSe_{1.71}$ as a function of magnetic fields parallel to (d) the *ab* plane and (e) the *c* axis at various temperatures. Despite the layered structure of the compound, the upper critical field is nearly isotropic, $\Gamma = 1.1$, in $Sn_{0.14}NbSe_{1.71}$. (f) Field dependence of the Hall resistivity of $Sn_{0.11}NbSe_{1.60}$ at 7 K ($H \parallel c, I \parallel ab$). The Hall resistivity ρ_{yx} is linear in H with the positive sign indicating that the hole band dominates the transport in $Sn_xNbSe_{2-\delta}$. The extracted Hall coefficient R_H from the slope of ρ_{yx} is 5.3×10^{-3} cm^3 C^{-1}, yielding a carrier density of 1.2×10^{21} cm^{-3}.
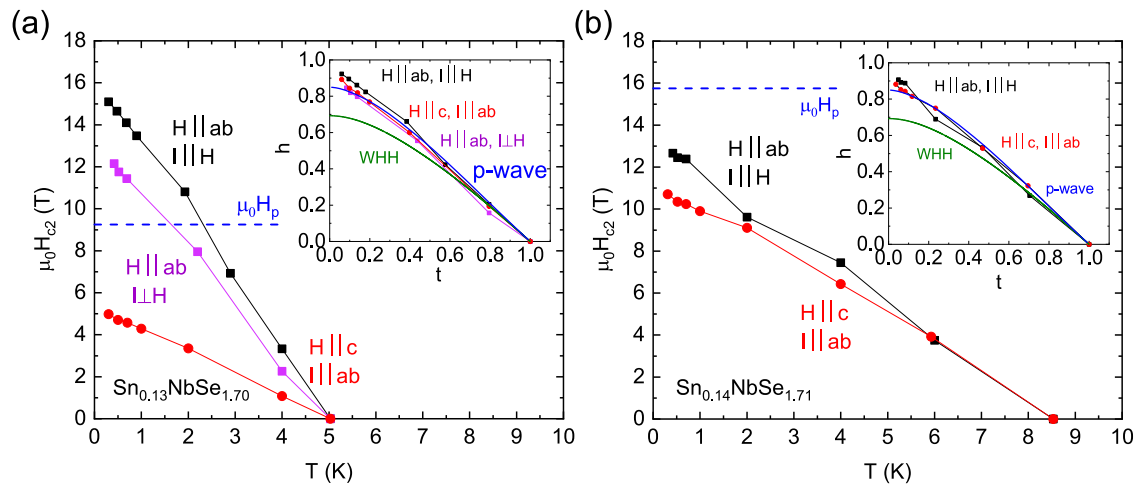
Figure 4. Temperature dependence and anisotropy of the upper critical field of $Sn_xNbSe_{2-\delta}$. (a) Temperature dependence of upper critical field determined by the midpoint of resistive transitions in figure 3 for $Sn_{0.13}NbSe_{1.70}$. Regardless of the field orientation, the upper critical field increases linearly with decreasing temperature down to 0.3 K. The zero-temperature values of in-plane upper critical fields $\mu_0H_{c2}^{ab}(0)$ for $H \parallel I$ and $H \perp I$ exceed the Pauli paramagnetic limit $\mu_0H_P = 1.84T_c = 9.3$ T, indicated by a blue dashed line. The zero-temperature value of out-of-plane $\mu_0H_{c2}^c(0)$ is lower than μ_0H_P. Inset: normalized upper critical field $h = H_{c2}/(-T_c dH_{c2}/dT|_{T=T_c})$ as a function of normalized temperature $t = T/T_c$ for $Sn_{0.13}NbSe_{1.70}$. For all the field orientations, the normalized upper critical field clearly deviates from the WHH model at low temperatures and is close to the calculation for the polar p-wave state [29]. (b) Temperature dependence of the upper critical field determined by the midpoint of resistive transitions in figure 3 for $Sn_{0.14}NbSe_{1.71}$. The upper critical fields for $H \parallel ab$ and $H \parallel c$ exhibit linear-in-temperature behavior down to 0.3 K. The zero-temperature values of in-plane and out-of-plane upper critical fields $\mu_0H_{c2}^{ab}(0)$ and $\mu_0H_{c2}^c(0)$ are lower than the Pauli paramagnetic limit $\mu_0H_P = 15.6$ T, indicated by a blue dashed line. Inset: normalized upper critical field h as a function of t for $Sn_{0.14}NbSe_{1.71}$. The normalized upper critical fields for both $H \parallel ab$ and $H \parallel c$ depart from the WHH model at low temperatures and are close to the calculation for the polar p-wave state [29].

linear in magnetic fields in the normal state above T_c, indicative of a dominant contribution to the charge transport from a large cylindrical hole band, around the Γ point, predicted by theoretical calculations [12, 28]. The slope of the Hall resistivity gives the Hall coefficient $R_H = 5.3 \times 10^{-3}$ cm^3 C^{-1}, hence the carrier density $n = 1.2 \times 10^{21}$ cm^{-3}.

The upper critical fields of $Sn_xNbSe_{2-\delta}$ exhibit quite unusual behavior, as shown in figure 4. With decreasing temperature starting from T_c, H_{c2} increases linearly in all the field configurations for both $Sn_{0.13}NbSe_{1.70}$ and $Sn_{0.14}NbSe_{1.71}$. The initial slopes of the upper critical fields parallel to the ab plane for $H \parallel I$, $dH_{c2}/dT|_{T=T_c}$, are -3.2 T/K for $Sn_{0.13}NbSe_{1.70}$ and -1.5 T/K for $Sn_{0.14}NbSe_{1.71}$, extremely larger than -0.19 K/T for $PbTaSe_2$ for $H \parallel ab$ [7]. The observed temperature dependence of H_{c2} for $Sn_xNbSe_{2-\delta}$ completely differs from those of conventional type-II superconductors. In conventional type-II superconductors, upper critical fields due to the orbital effect are explicated by the WHH theory [22]. In the WHH theory, the zero-temperature value of upper critical field can be written as $H_{c2}(0) = -\alpha T_c dH_{c2}/dT|_{T=T_c}$, where α is 0.69 for the dirty limit and 0.73 for the clean limit [22]. However, as shown in the insets to figures 4(a) and (b), the normalized upper critical field $h = H_{c2}/(-T_c dH_{c2}/dT|_{T=T_c})$ strikingly deviates from the WHH values and is close to the calculations for the polar p-wave state [29]. The extracted α for $Sn_xNbSe_{2-\delta}$ is ~ 1.0.

Equally unusual in $Sn_xNbSe_{2-\delta}$ are the magnitudes of the upper critical fields. The zero temperature value of the in-plane upper critical field $\mu_0H_{c2}^{ab}(0)$ for $Sn_{0.13}NbSe_{1.70}$ is ~ 16 T, exceeding the Pauli paramagnetic limit $\mu_0H_P = 1.84T_c =$

9.3 T obtained from a simple estimation within the weak-coupling BCS theory with $2\Delta = 3.5k_BT_c$ (figure 4(a)) [30]. The persistence of superconductivity beyond the BCS Pauli paramagnetic limit suggests a possible odd-parity contribution in the superconducting gap function, as found in non-centrosymmetric heavy fermions superconductor $CePt_3Si$ [31] and metal-intercalated Bi_2Se_2 [32].

In $Sn_{0.14}NbSe_{1.71}$, $\mu_0H_{c2}^{ab}(0)$ is 13 T, comparable to but slightly lower than $\mu_0H_P = 15.6$ T enhanced by the higher T_c of 8.6 K (figure 4(b)). The zero temperature values of out-of-plane upper critical fields $\mu_0H_{c2}^c(0)$ of $Sn_xNbSe_{2-\delta}$ are lower than the Pauli paramagnetic limit. Utilizing the Ginzburg–Landau relation, $\mu_0H_{c2}^c(0) = \phi_0/2\pi\xi_{ab}^2$ and $\mu_0H_{c2}^{ab}(0) = \phi_0/2\pi\xi_c\xi_{ab}$, where ϕ_0 is the magnetic flux quantum, we can estimate the coherence lengths: $\xi_{ab} = 15$ nm and $\xi_c = 4.5$ nm for $Sn_{0.13}NbSe_{1.70}$ and $\xi_{ab} = 5.0$ nm and $\xi_c = 6.0$ nm for $Sn_{0.14}NbSe_{1.71}$.

Although our observations suggest the presence of a possible odd-parity contribution to the pairing states at least in $Sn_{0.13}NbSe_{1.70}$ with T_c of 5.0 K, its superconductivity is robust against scattering due to nonmagnetic disorder. In general, nonmagnetic scattering strongly suppresses unconventional superconductivity [33], including odd-parity pairing states, as described by the Abrikosov–Gor'kov model [34]. The Abrikosov–Gor'kov model shows that T_c of unconventional superconductors are dramatically suppressed to zero by nonmagnetic scattering, as the mean free path ℓ becomes comparable to the coherence length, $\xi \sim \ell$. To estimate the mean free paths in $Sn_xNbSe_{2-\delta}$, we exploit the Hall effect, along with electrical resistivity. Assuming a single cylindrical hole band,

we can extract mean free paths by using $\ell = (\hbar/\rho e^2)\sqrt{2\pi c/n}$, where c is the lattice constant along the c axis. The extracted mean free paths at T_c are $\ell = 5.9$ nm for $Sn_{0.13}NbSe_{1.70}$ and 3.1 nm for $Sn_{0.14}NbSe_{1.71}$. Here we have used the carrier density n from the Hall coefficient for $Sn_{0.11}NbSe_{1.60}$. Surprisingly, these values are much smaller than the coherence lengths in the ab plane, intuitively inconsistent with the possible odd-parity pairing state.

However, there is a precedence in which odd-parity superconductivity was found to be invulnerable to nonmagnetic disorder—metal-intercalated Bi_2Se_3 [17, 32, 35]. In this topological superconductor, the robustness of the odd-parity superconductivity is thought to be due to strong spin–orbit coupling [36, 37]. Similarly, nonnegligible spin–orbit coupling due to Sn, a relatively heavy element, may be protecting superconductivity in $Sn_xNbSe_{2-\delta}$ against strong nonmagnetic scattering. The shared features of superconductivity in the two compounds—the upper critical fields beyond the Pauli paramagnetic limit and the robust superconductivity against disorder—possibly suggest that the odd-parity superconductivity is realized in $Sn_xNbSe_{2-\delta}$.

We briefly comment on a possible nematic superconducting state in the $PbTaSe_2$ family. Nematic superconductivity, accompanied by a rotational symmetry breaking in the superconducting state, is observed in metal-intercalated Bi_2Se_3, evidencing topological superconductivity in the system [38–41]. Similarly, in $PbTaSe_2$, soft point-contact spectroscopy [42] elucidates the rotational symmetry breaking in superconducting properties, possibly associated with nematic superconductivity. In $Sn_{0.13}NbSe_{1.70}$, we observe clear anisotropy in in-plane upper critical fields for two different configurations, $H \parallel I$ and $H \perp I$, as shown in figure 4(a). However, the measured anisotropy can be attributed to the presence/absence of flux flow due to the Lorentz force as observed in MgB_2 [43], masking intrinsic twofold symmetry associated with electronic nematicity in this system, if present. Indeed, we observe kinks in the resistive transition associated with vortex motion due to the Lorentz force only in the $H \perp I$ configuration as shown in figure 3(c) [44]. To determine the intrinsic in-plane anisotropy, further experimental investigations will be required.

In summary, we have grown single crystals of $Sn_xNbSe_{2-\delta}$ with a noncentrosymmetric crystal structure, and found superconductivity with relatively high T_c, 8.6 K, among known topological superconductor candidates. The upper critical field of $Sn_{0.13}NbSe_{1.70}$, with $T_c = 5$ K, exceeds the Pauli paramagnetic limit, suggestive of a possible contribution of odd-parity pairing in the superconductivity. The possible odd-parity pairing component, a prerequisite for topological superconductivity, makes this system a promising material for further study.

Acknowledgments

Data availability statement

The data that support the findings of this study are available upon reasonable request from the authors.

ORCID iDs

Yasuyuki Nakajima ![ORCID] https://orcid.org/0000-0002-4584-3621

References

[1] Sato M and Ando Y 2017 *Rep. Prog. Phys.* **80** 076501
[2] Kitaev A Y 2003 *Ann. Phys., NY* **303** 2
[3] Nayak C, Simon S H, Stern A, Freedman M and Das Sarma S 2008 *Rev. Mod. Phys.* **80** 1083
[4] Harada S, Zhou J J, Yao Y G, Inada Y and Zheng G-q. 2012 *Phys. Rev.* B **86** 220502
[5] Ali M N, Gibson Q D, Klimczuk T and Cava R J 2014 *Phys. Rev.* B **89** 020505
[6] Long Y-J, Zhao L-X, Wang P-P, Yang H-X, Li J-Q, Zi H, Ren Z-A, Ren C and Chen G-F 2016 *Chinese Phys. Lett.* **33** 037401
[7] Zhang C-L, Yuan Z, Bian G, Xu S-Y, Zhang X, Hasan M Z and Jia S 2016 *Phys. Rev.* B **93** 054520
[8] Wang M X, Xu Y, He L P, Zhang J, Hong X C, Cai P L, Wang Z B, Dong J K and Li S Y 2016 *Phys. Rev.* B **93** 020503
[9] Pang G M *et al* 2016 *Phys. Rev.* B **93** 060506
[10] Bian G *et al* 2016 *Nat. Commun.* **7** 10556
[11] Chang T-R *et al* 2016 *Phys. Rev.* B **93** 245130
[12] Chen P-J, Chang T-R and Jeng H-T 2016 *Phys. Rev.* B **94** 165148
[13] Butch N P, Syers P, Kirshenbaum K, Hope A P and Paglione J 2011 *Phys. Rev.* B **84** 220504
[14] Nakajima Y *et al* 2015 *Sci. Adv.* **1**
[15] Sasaki S, Ren Z, Taskin A A, Segawa K, Fu L and Ando Y 2012 *Phys. Rev. Lett.* **109** 217004
[16] Hor Y S *et al* 2010 *Phys. Rev. Lett.* **104** 057001
[17] Kriener M, Segawa K, Ren Z, Sasaki S and Ando Y 2011 *Phys. Rev. Lett.* **106** 127004
[18] Liu Z, Yao X, Shao J, Zuo M, Pi L, Tan S, Zhang C and Zhang Y 2015 *J. Am. Chem. Soc.* **137** 10512
[19] Imai Y, Nabeshima F, Yoshinaka T, Miyatani K, Kondo R, Komiya S, Tsukada I and Maeda A 2012 *J. Phys. Soc. Japan* **81** 113708
[20] Liu P-F, Li J, Tu X-H, Yin H, Sa B, Zhang J, Singh D J and Wang B-T 2020 *Phys. Rev.* B **102** 155406
[21] Beenakker C W J 2015 *Rev. Mod. Phys.* **87** 1037
[22] Werthamer N R, Helfand E and Hohenberg P C 1966 *Phys. Rev.* **147** 295
[23] Momma K and Izumi F 2011 *J. Appl. Cryst.* **44** 1272
[24] Gentile P S, Driscoll D A and Hockman A J 1979 *Inorg. Chim. Acta* **35** 249
[25] Naik S, Pradhan G K, Bhat S G, Behera B C, Kumar P S A, Samal S L and Samal D 2019 *Physica* C **561** 18
[26] Karnezos N, Welsh L B and Shafer M W 1975 *Phys. Rev.* B **11** 1808
[27] Sankar R, Rao G N, Muthuselvam I P, Chang T-R, Jeng H T, Murugan G S, Lee W-L and Chou F C 2017 *J. Phys.: Condens. Matter.* **29** 095601
[28] Xu X, Kang Z, Chang T-R, Lin H, Bian G, Yuan Z, Qu Z, Zhang J and Jia S 2019 *Phys. Rev.* B **99** 104516
[29] Scharnberg K and Klemm R A 1980 *Phys. Rev.* B **22** 5233

[30] Clogston A M 1962 *Phys. Rev. Lett.* **9** 266
[31] Bauer E *et al* 2004 *Phys. Rev. Lett.* **92** 027003
[32] Bay T V, Naka T, Huang Y K, Luigjes H, Golden M S and de Visser A 2012 *Phys. Rev. Lett.* **108** 057001
[33] Mackenzie A P, Haselwimmer R K W, Tyler A W, Lonzarich G G, Mori Y, Nishizaki S and Maeno Y 1998 *Phys. Rev. Lett.* **80** 161
[34] Abrikosov A A and Gor'kov L P 1960 *Zh. Éksp. Teor. Fiz.* **39** 1781
Abrikosov A A and Gor'kov L P 1961 *Sov. Phys. JETP* **12** 1243 (Engl. transl.)
[35] Sasaki S, Kriener M, Segawa K, Yada K, Tanaka Y, Sato M and Ando Y 2011 *Phys. Rev. Lett.* **107** 217001
[36] Michaeli K and Fu L 2012 *Phys. Rev. Lett.* **109** 187003
[37] Nagai Y, Ota Y and Machida M 2014 *Phys. Rev. B* **89** 214506
[38] Matano K, Kriener M, Segawa K, Ando Y and Zheng G-q 2016 *Nat. Phys.* **12** 852
[39] Pan Y, Nikitin A M, Araizi G K, Huang Y K, Matsushita Y, Naka T and de Visser A 2016 *Sci. Rep.* **6** 28632
[40] Smylie M P *et al* 2017 *Phys. Rev. B* **96** 115145
[41] Yonezawa S, Tajiri K, Nakata S, Nagai Y, Wang Z, Segawa K, Ando Y and Maeno Y 2017 *Nat. Phys.* **13** 123
[42] Le T *et al* 2020 *Sci. Bull.* **65** 1349
[43] Shi Z X, Tokunaga M, Tamegai T, Takano Y, Togano K, Kito H and Ihara H 2003 *Phys. Rev. B* **68** 104513
[44] Zhu X D, Lu J C, Sun Y P, Pi L, Qu Z, Ling L S, Yang Z R and Zhang Y H 2010 *J. Phys.: Condens. Matter.* **22** 505704